Gait & Posture 60 (2018) 279–285

Contents lists available at ScienceDirect

Gait & Posture

journal homepage: www.elsevier.com/locate/gaitpost

ESMAC best paper 2016

A methodological framework for detecting ulcers' risk in diabetic foot subjects by combining gait analysis, a new musculoskeletal foot model and a foot finite element model

Alessandra Scarton[a,1], Annamaria Guiotto[a,1], Tiago Malaquias[b,1], Fabiola Spolaor[a], Giacomo Sinigaglia[a], Claudio Cobelli[a], Ilse Jonkers[c], Zimi Sawacha[a,*]

[a] Department of Information Engineering, University of Padova, Via Gradenigo 6b, Padova, 35131, Italy
[b] Department of Mechanical Engineering, Biomechanics Section, Celestijnenlaan 300-box 2419, 3001 Leuven, Belgium
[c] Department of Kinesiology, Human Movement Biomechanics Research Group, KU Leuven, Tervuursevest 101 – Box 1501, 3001, Leuven, Belgium

ARTICLE INFO

Keywords:
Diabetic foot prevention
Muscle forces
Musculoskeletal modelling
Finite element modelling
Multisegment foot model

ABSTRACT

Diabetic foot is one of the most debilitating complications of diabetes and may lead to plantar ulcers. In the last decade, gait analysis, musculoskeletal modelling (MSM) and finite element modelling (FEM) have shown their ability to contribute to diabetic foot prevention and suggested that the origin of the plantar ulcers is in deeper tissue layers rather than on the plantar surface. Hence the aim of the current work is to develop a methodology that improves FEM-derived foot internal stresses prediction, for diabetic foot prevention applications. A 3D foot FEM was combined with MSM derived force to predict the sites of excessive internal stresses on the foot. In vivo gait analysis data, and an MRI scan of a foot from a healthy subject were acquired and used to develop a six degrees of freedom (6 DOF) foot MSM and a 3D subject-specific foot FEM. Ankle kinematics were applied as boundary conditions to the FEM together with: 1. only Ground Reaction Forces (GRFs); 2. *OpenSim* derived extrinsic muscles forces estimated with a standard *OpenSim* MSM; 3. extrinsic muscle forces derived through the (6 DOF) foot MSM; 4. intrinsic and extrinsic muscles forces derived through the 6 DOF foot MSM. For model validation purposes, simulated peak pressures were extracted and compared with those measured experimentally. The importance of foot muscles in controlling plantar pressure distribution and internal stresses is confirmed by the improved accuracy in the estimation of the peak pressures obtained with the inclusion of intrinsic and extrinsic muscle forces.

1. Introduction

A sensorimotor polyneuropathy is a long-term diabetic complication. The main consequences are plantar ulcers and lower limb amputations which is a major cause of morbidity and mortality [1]. The prevalence of diabetic sensorimotor polyneuropathy in diabetic patients is 25% after 10 years of disease, and it is often associated with peripheral artery disease. Diabetic foot ulcers are commonly due to repetitive stress over an area that is subject to high vertical or shear stress in patients with peripheral neuropathy and peripheral artery disease. Several preventive approaches have been proposed [1] including clinical and biomechanical interventions [1–13]. Biomechanical analysis has been carried out using experimental and computational methods, via Finite Element models (FEMs) or Musculoskeletal models (MSMs). Despite the advances in prevention methodologies, there is an increasing number of diabetic foot subjects and lower extremity amputations [1].

Experimental studies report that diabetic neuropathy significantly reduces walking ability and causes alterations of foot posture and function [2–8]. Limited foot flexibility and a restrained forward progression of body weight during the stance phase of gait were observed [2–4]. As a consequence, balance is impaired and the risk of falls increased [2,5,8]. An inadequate foot rollover associated with a smaller ankle range of motion modifies the plantar pressure (PP) distribution inducing higher PP concentration and a higher risk for ulcer formation at specific foot areas [2,3,5,6]. Diabetes also accelerates age-related

* Corresponding author.
E-mail addresses: alessandra.scarton@gmail.com (A. Scarton), annamaria.guiotto@dei.unipd.it (A. Guiotto), melo.malaquias@kuleuven.be (T. Malaquias), fabiola.spolaor@unipd.it (F. Spolaor), giacomos404@gmail.com (G. Sinigaglia), cobelli@dei.unipd.it (C. Cobelli), ilse.jonkers@faber.kuleuven.be (I. Jonkers), zimi.sawacha@dei.unipd.it (Z. Sawacha).
[1] These authors have contributed equally to this work.

http://dx.doi.org/10.1016/j.gaitpost.2017.08.036
Received 28 August 2017; Accepted 30 August 2017

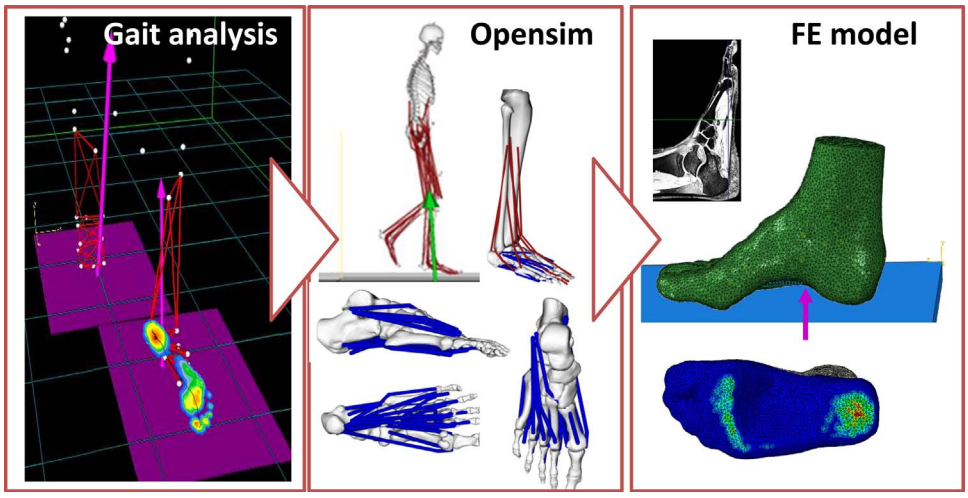

Fig. 1. Workflow of the adopted procedure: step1 (left) acquisition of 3D foot kinematics and kinetics during gait analysis; step 2 (centre) MSM in order to provide muscle forces; step 3 (right) foot FEM for simulation of internal stresses and strains, and plantar pressure.

decreases in muscle mass [4] contributing to electromyographic abnormalities in the lower limb muscles [6,7]. Recently, strengthening, stretching and functional training programmes are being combined with the use of insoles to reduce the stress of the plantar tissue [5].

Current literature shows that ulceration seems to be caused by repetitive and/or excessive mechanical loading on the surface of the insensitive skin, which leads to tissue damage. Clinical studies have indicated that prediction of ulcer risk level can be substantially improved when static and dynamic PP measurements are performed [2–4,5,8]. However, it should be mentioned that while experimental techniques can only assess loading at the foot–ground interface, reliable numerical models can provide insight on internal stresses and strains tolerated by the plantar and even deeper foot tissue [9–14]. Different foot FEMs have been developed that account for critical aspects of the diabetic foot [9–14]. The model developed by Gefen et al. (2003) [11] revealed significant tension stress concentrations, known as von Mises stresses, in the plantar pad of the simulated diabetic forefoot, as high as four times the normal maximum stress under the first metatarsal head and almost eight times under the second metatarsal head. The increased internal stresses at the plantar soft tissue suggest that injury onset in diabetic feet is in the deeper tissue layers rather than on the plantar foot surface. Thus, there is a need for further investigation of the aetiopathogenesis of diabetic foot through FEM.

Furthermore, while PP can be directly measured through PP sensors, there is not an experimental gold standard available for internal stress measurements. Therefore the comparison between FEM derived PP, and experimentally measured PP, is used as the standard validation method [13].

The majority of foot FEMs rely on the use of a simplified or partial foot shape, linear material properties and non subject-specific boundary conditions. When limiting these assumptions by using a subject specific 3D FEM combined with subject specific gait analysis data [13], the authors validated their model through direct comparison with the experimentally measured peak PP acquired during gait on the same subject, reaching an error of 18% and 36% respectively in the healthy and diabetic subjects' simulated PP.

The use of MSMs has proliferated in the biomechanics community thanks to its ability to evaluate muscle and joint contact forces during gait [15–18]. However, we are unaware of FEM studies evaluating the influence of muscle forces on the PP distribution during gait. Given the recent focus on muscle retraining exercises as part of rehabilitation programmes [5], such insights may be invaluable in defining targeted training programmes in neuropathic subjects.

The aim of this study was to develop a methodology for improving the prediction of internal stresses and strain on the foot through a 3D FEM based on subject specific gait analysis data combined with MSM derived intrinsic and extrinsic foot muscle forces. The feasibility of the pipeline was verified using the integrated motion capture data of one healthy subject. The model was validated through direct comparison between the simulated PP distribution and the coinciding experimentally measured ones. Finally, the role of the foot muscles on the internal stress distribution was evaluated by comparing estimates of foot models with different levels of complexity and muscle detail.

2. Methods

The framework follows three consecutive steps (Fig. 1): 1) Integrated 3D motion capture. 2) Calculation of muscle forces using MSMs and 3) Calculation of PP and stresses in soft tissues and bones using FEMs.

Subject specific data from one healthy subject (female, age 31 years, BMI 20.1 kg/m^2) was used through the whole modelling procedure. The subject gave written informed consent. The protocol was approved by the local Ethic Committee of the University Clinic of Padova [13].

2.1. Gait analysis

An integrated motion capture set-up was used consisting of a 6 cameras stereophotogrammetric system, (60 Hz, BTS S.r.l, Italy), 2 force plates (960 Hz, FP4060-10, Bertec Corporation, USA), 2 PP systems (41 × 41 cm, 0.64 cm^2 resolution, 150 Hz, Imagortesi, Italy), and a 12-channel surface electromyography system (FreeEmg1000, BTS, 1000 Hz). Electromyography activity of Tibialis Anterior, Gastrocnemius Lateralis, Rectus Femoris, Gluteus Medius, Extensor Digitorum Comunis and Peroneus Lateralis was acquired. A multi-segment foot model [3] and a full body marker set [19] were combined. The full body marker set was used for the *OpenSim* scaling procedure and for defining muscle insertion points; the multi-segment foot model was used for providing the anatomical landmarks (ALs) co-ordinates necessary to develop the 8 DOF MSM of the foot [20], and to determine the FEM boundary conditions [13]. One static trial was collected, with the subject standing with his feet 30° apart and his arms along the body. Several walking trials were collected at self-selected speed; at least three walking trials with three right and three left foot contacts on both the force and pressure plates were collected [3].

2.2. MSM

All raw data was converted into a format compatible with *OpenSim* using MOtoNMS [21]. A generic MSM (GaitModel 2392) with 10 rigid bodies, 23 DOF and 92 musculo-tendon actuators was scaled using markers placed on ALs during a static trial and experimentally

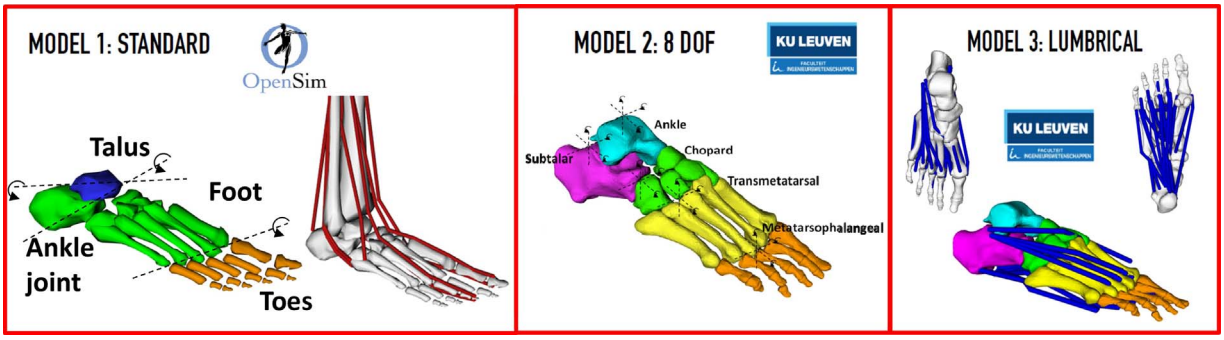

Fig. 2. *OpenSim* foot MSMs used in the step 2: Model 1 is the standard *OpenSim* foot model with all the extrinsic foot muscles (medial gastrocnemius, lateral gastrocnemius, soleus, tibialis posterior, tibialis anterior, peroneus brevis, peroneus longus, extensor digitorum, extensor hallucis were included in the FEM: SM1); Model 2 is the recently proposed 8 degrees of freedom *OpenSim* foot model with the extrinsic muscles (same as model 1: SM2); Model 3 is the same as Model 2 but includes all the intrinsic foot muscles (abductor hallucis, quadratus plantae, flexor digitorum, flexor hallucis were included in the FEM: SM3).

measured body mass in order to match the subject's dimensions and inertial properties [15].

Three different foot definitions were included in the MSM:

Model 1 (M1) included the standard 3 DOF, *OpenSim* foot model (Simulation with M1–SM1) (Fig. 2-left), containing the talus, foot (rigid segment grouping calcaneus, navicular, cuneiforms, cuboid and metatarsals) and toes (rigid segment grouping the proximal and distal phalanges). The 3 DOF are plantarflexion/dorsiflexion in the ankle and in the metatarsophalangeal joint and eversion/inversion in the subtalar joint. The model includes the extrinsic foot muscles [15].

Model 2 (M2) with a 8 DOF *OpenSim* foot model [20] and the extrinsic muscles (Simulation with M2–SM2, Fig. 2-centre): The model includes five foot segments (being calcaneus, talus, midfoot, forefoot and toes) and: 1 DOF at the ankle joint, e.g., plantarflexion/dorsiflexion, 1 DOF at the subtalar joint, e.g. eversion/inversion; 2 DOF at the midtarsal joint both allowing a combination of eversion-abduction-extension/inversion-adduction-flexion; 2 DOF at the tarsometatarsal joint, both allowing flexion-eversion/extension-eversion; 2 DOF at the metatarsophalangeal joint e.g. plantarflexion/dorsiflexion and adduction/abduction [20]. In the absence of markers on the toes, the latter was locked therefore reducing the model to 6 DOF (and it will be further referred to as 6 DOF).

Model 3 (M3) also included the intrinsic foot muscles in the 6 DOF foot model (Simulation with M3–SM3, Fig. 2-right): Only the intrinsic muscles with origin, insertion and via points in two or more of the five segments were included [20,22,23] and were modelled using the "Path Actuator" – *OpenSim*'s class, which describes the muscle force as a ratio of an optimal force transferred to the interconnected bodies via a geometrical path [15].

Based on each of the three scaled MSMs, simulations of three gait trials were generated in *OpenSim* (v.3.2) [15] to calculate the underlying muscle forces using the static optimization algorithm [15]. Given the multi-segment foot definition in M2 and M3, the GRFs were subdivided according to the number of foot segments using an ad hoc developed algorithm based on the PP data [22].

Simulated muscles' activation peak position within the stance phase of gait was compared with the corresponding experimentally derived one, for validation purposes.

2.3. FEM

The right foot MRI was acquired in an unloaded condition using a 1.5 T MRI scan (Philips Achieva, spacing between slices: 0.6 mm and slice thickness: 1.2 mm, sequence 3D mFFE, TE/TR 9/33). An angle between foot and leg of 90° was maintained with the help of pillows on the sides of the limb. The grey-scale-images were then segmented (Simpleware-ScanIP v.5.0) to obtain the geometries of 30 bones and of the skin as contour of the foot soft-tissues' homogenous mass. The model was developed as in [11] and consisted of a volume mesh of 34800 elements imported in *Abaqus*. Material properties were assigned for each element from the literature [11]. Muscle insertions were identified in the MRI using anatomical atlases [23,24], while muscles and ligaments were represented using connectors between origin and insertion. More specifically Tibialis Anterior, Tibialis Posterior, Peroneus Brevis, Peroneus Longus, Medial and Lateral Gastrocnemius, Soleus, Extensor Hallucis Longus and Brevis and Extensor Digitorum Longus and Brevis were added, as well as the calcaneonavicular, long plantar and calcaneocuboid ligaments and the plantar fascia (Fig. 3). Muscles characterized by a large area of insertion (e.g. soleus and gastrocnemius) as well as the plantar fascia were represented by multiple connectors to evenly spread the loads [25]. Muscles that were not visible in the foot MRI were defined with respect to the coordinates of the relevant ALs as in the MSM. In addition, the intrinsic muscles, were represented using specific connectors.

The position of the foot over the platform was determined using the experimental co-ordinates of the foot ALs. The whole foot vertical GRF and the 3D foot angles relative to the global reference system were combined as boundary conditions together with the muscles' force computed in the *OpenSim* static optimization [26]. The superior surfaces of the tibia, fibula and soft-tissue were completely fixed to simulate the effects of constraints from superior-lying tissues [13].

A quasi-static analysis was performed considering 4 instants of the stance phase of the gait cycle [11], specifically Initial Contact ((IC) 1% of the stance), Loading Response ((LR) 30% of the stance), Mid-stance ((MS) 50% of the stance) and Push-Off ((PO) 92% of the stance). For these instances, simulations were run using muscle forces calculated from the 3 models (SM1, SM2, SM3), and by only applying the GRF (SGRF).

The simulation error, for the peak PP, was calculated as the difference between simulated and experimental data and expressed as a percentage of the experimental one [11], with the simulated data being the contact pressure at the plate nodes, the contact stresses at foot–supporting interface and Von Mises stresses in the bones and the soft tissues. The latter was previously considered a parameter related to the strength of biological tissues of bone and plantar soft-tissue [11].

3. Results

Results of peak PP and Von Mises were reported in Figs. 4 and 5 for the four different boundary conditions. In order to verify the accuracy of each simulated condition, the experimentally measured PP was compared with the simulated one (Fig. 4).

The highest experimental PP was revealed at LR on the hindfoot (504.4KPa), and SM1 and SM3 provided the best estimate with an error of 5.3% and 10.8% respectively.

At IC, the peak PP measured at the hindfoot (204.8KPa) was well

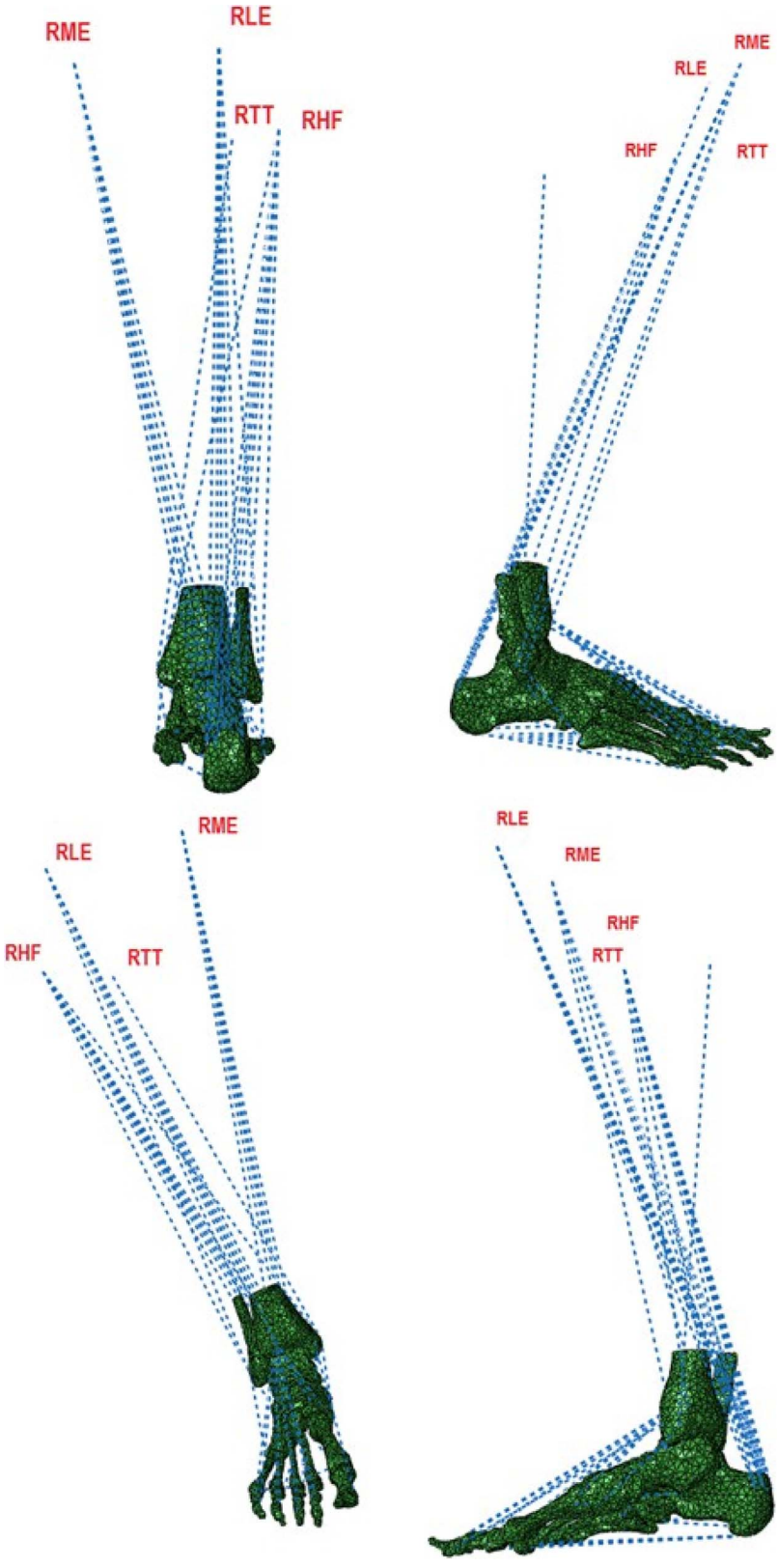

Fig. 3. Example of one of the foot FEM with wires connectors representing muscles: frontal posterior and lateral views.

approximated by all simulations, with SM3 having the highest resemblance (2.5% error). During LR and MS, PP increases, shifting loading towards midfoot and forefoot. At LR simulated peak PP ranged between 477.5KPa (SM1-hindfoot) and 0 KPa (SGRF-forefoot), while experimental peak PP ranged between 504.4KPa (hindfoot) and 22.4KPa (midfoot). At MS simulated peak PP ranged between 484.2KPa (SM2-forefoot) and 70.1KPa (SM1-midfoot), while experimental PP ranged between 331KPa (forefoot) and 192KPa (midfoot). With the exception of SM2 in the forefoot, all other approaches underestimated the PP and obtained similar results. During PO, PP is born by the forefoot only; simulated PP ranged between 1316.4KPa (SM1-forefoot) and 24.7KPa (SGRF-midfoot); 196 KPa were the experimental PP registered only on

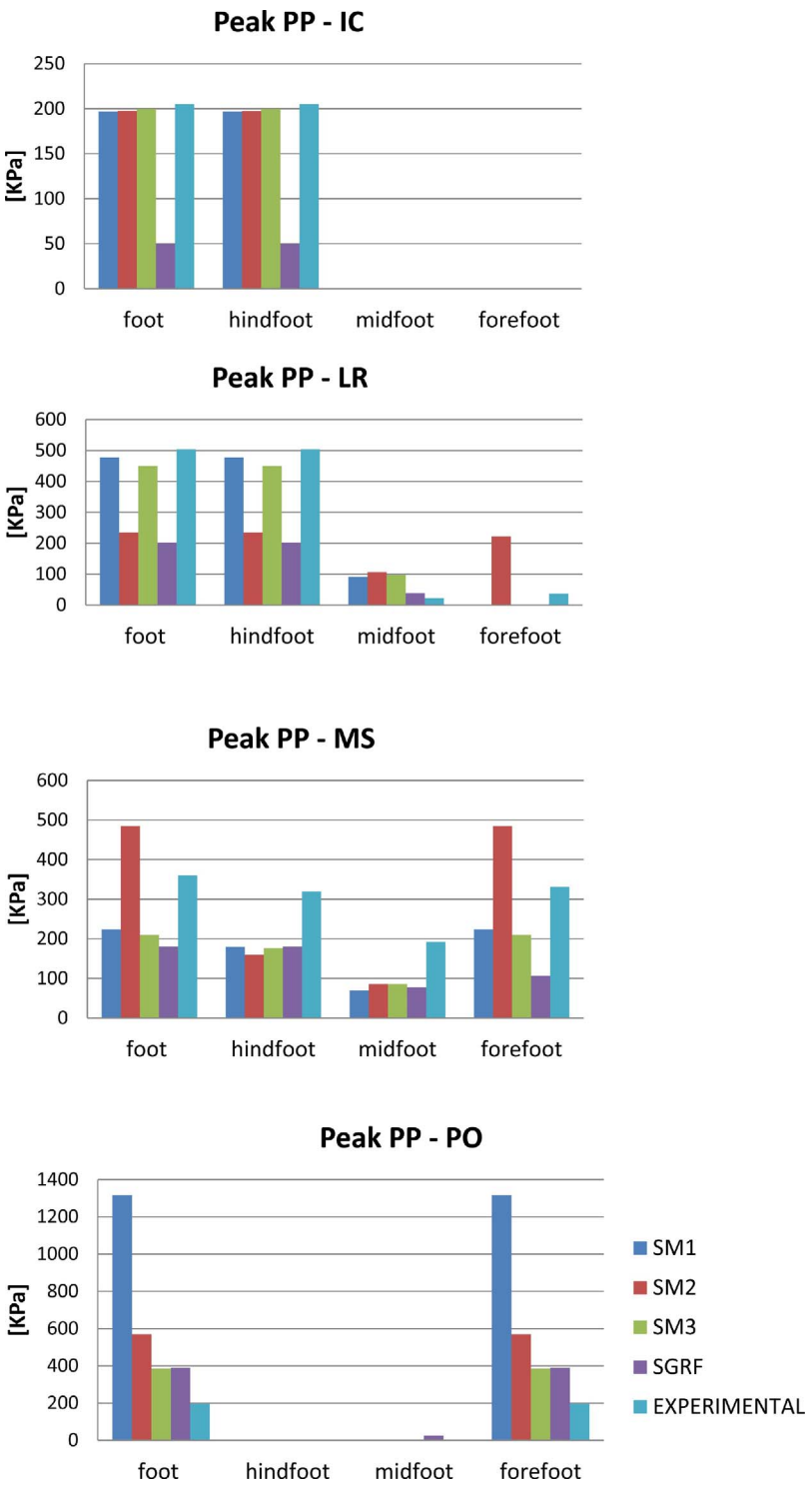

Fig. 4. Peak and mean plantar pressure (PP): comparison between the experimental and the simulated PP in the 4 modelling conditions (SM1, SM2, SM3, SMGRF). For correspondence please refer to the legend in the figure.

the forefoot. All modelling approaches overestimated the peak PP, with SM1 presenting the largest error (571% on the forefoot).

During gait, relatively high von Mises stresses were predicted at the bones in particular on both the metatarsals heads and the phalanxes especially the 1st, 3rd and 4th. The highest Von Mises stress in the bones was registered in the SM1 (79 MPa during the PO) even though this simulation was in poorest agreement with the experimental PP. Peak bone stress was found at the forefoot in all simulation conditions with a stress reduction up to 31 MPa and 8 MPa respectively in SM2 and SM3. Moreover SM3 revealed lower Von Mises stresses while providing the best prediction of the experimental PP.

The highest Von Mises stress in the soft tissue was obtained at the heel during LR (1 MPa). Similarly a reduction was obtained through the more complex models respectively up to 0.86 MPa and 0.8 MPa in SM2 and SM3.

An overall agreement was found between MSM extrinsic foot muscles' peaks of activation positions within the stance phase of gait and the corresponding experimentally derived ones.

4. Discussion

The goal of the present study was to develop a methodology to

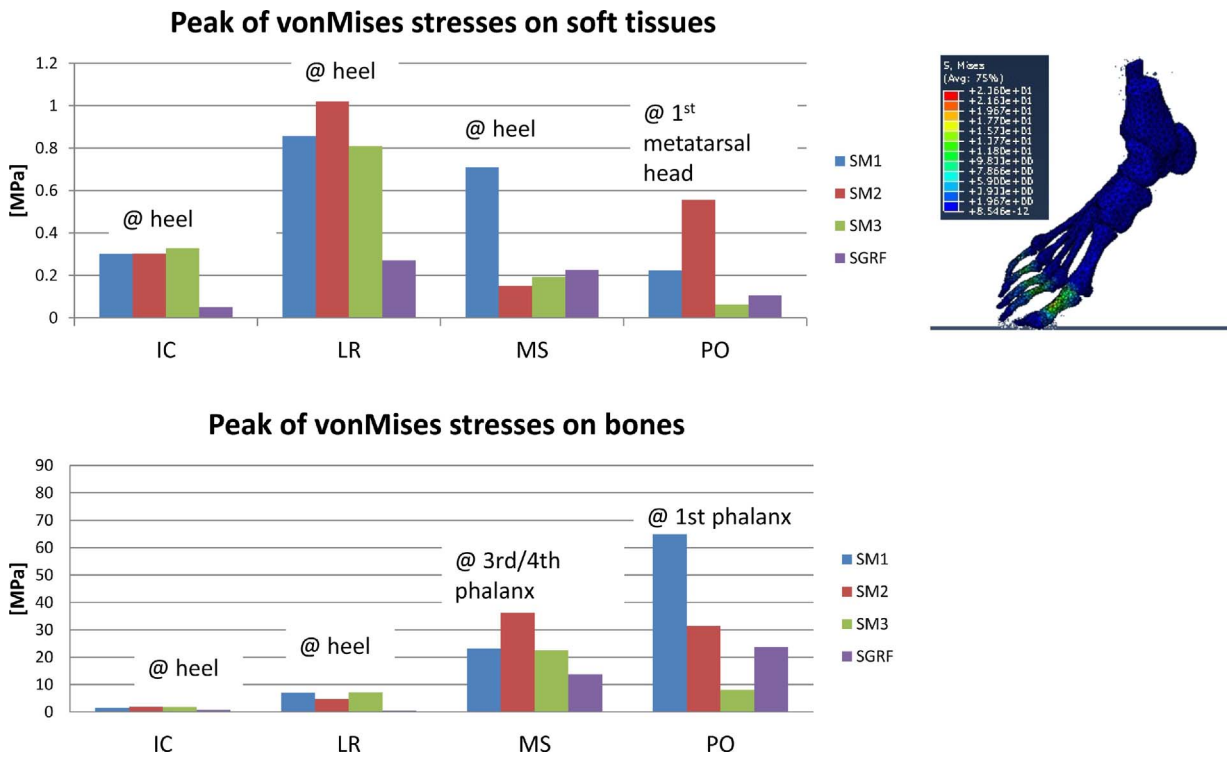

Fig. 5. Von Mises stresses: results of the Von Mises stresses estimated through the simulations performed in the 4 modelling conditions (SM1, SM2, SM3, SMGRF) and in the 4 instants of the stance phase of gait: initial contact (IC), loading response (LR), midstance (MS) and pushoff (PO). For correspondence please refer to the legend in the figure. In the upper right corner an example of Von Mises distribution on the 3D foot FEM can be observed.

improve the prediction of internal stresses and strain on the foot for future diabetic foot prevention purposes whilst investigating the effect of different modelling techniques on internal stress estimation. The validity of the application of the different model parameters related to foot model complexity as well as the inclusion of intrinsic muscle forces was assessed through direct comparison between simulated and experimentally measured PP.

In general, SM3 represented the most accurate solution, comparable to the results of Antunes et al. [30] who estimated a maximum pressure of 111 KPa in the heel, with a static balance test. The better agreement for the simulations using muscle forces as boundary conditions was already reported in the study of Chen et al. [11] who showed that inclusion of Soleus and Gastrocnemius were crucial for an appropriate estimation of the peaks of pressure [14].

In general, the calculated peak PP was underestimated, with the lowest error between simulated and experimental PP being 2.5% in SM3 at IC, and with the highest error being 571.6% in SM1 at PO. The lowest error was obtained with the most complex model including 6 DOF and both intrinsic and extrinsic foot muscles, while the worst prediction was determined with the more general model.

At the bone level, the highest Von Mises stresses were found on the 3rd/4th phalanxes in MS and the 1st in PO, for SM1 followed by SM2 and SM3 (Fig. 5), reaching a maximum of 79 MPa (SM1 in PO), 36.1 MPa (SM2 in MS), 22 MPa (SM3). These results are comparable with those reported in [11,12,14,25] and might be useful for future diabetic foot prevention applications such as early detection of onset and development of foot injuries.

The peak Von Mises stresses at the soft tissue level were found at the heel during IC, LR and MS and in correspondence of the 1st metatarsal head during PO. This will be even more relevant in the case of diabetic foot subjects that frequently display plantar ulcers at the forefoot and heel [1,9–11].

In SM1 peak Von Mises stress varied from 0.8 MPa to 0.2 MPa, while in SM2 and SM3 they varied respectively from 1 MPa to 0.1 MPa and from 0.8 MPa to 0.06 MPa. Again SM3 yielded lower Von Mises stresses.

The use of boundary conditions obtained from MSMs with different model complexity allowed evaluation of the effect of the intrinsic muscles on the internal stress distribution in the foot. Indeed, SM3 prediction was found to be more accurate during MS and PO, and estimated lower internal stresses, compared to SM2. Based on this observation it can be concluded that extrinsic and intrinsic foot muscles affect the forefoot force transmission at both the MS and the PO, and that there is a reduction in internal stresses and PP when intrinsic muscles are taken into account. This is further confirmed when considering the lower Von Mises stresses at the soft tissue level in SM3.

A similar spatial distribution of peak PP and internal stresses was observed at IC and PO (Figs. 5 and 4) while this was not confirmed at the bones during the LR and at the tissue level during the MS. Hence it could be hypothesized that in some cases excessive internal stresses precede the onset of excessive PP; this could explain why plantar ulcers do not always occur on those foot sites where peak PP were registered. However the framework should be applied to diabetic foot patients to confirm this hypothesis.

Limitations of the present study should not be ignored and might be responsible for the differences registered between experimental and simulated pressures in particular at PO (SM1). Material properties were taken from the literature and muscle forces have been implemented as connectors in the FEM [13,25]. Foot kinematic data was captured using surface markers and skin artefact may be an issue [28,29], however invasive measurements [29] and exposure to treatment [28] are needed to overcome this problem. With respect to MRI acquisition, the foot geometry was acquired in an unloaded position [11], in order to avoid deformation of the foot which would lead to unknown loading conditions for the FEM. Theoretically this could be overcome by measuring plantar soft tissue compressive force simultaneously with the MRI [27], but this is not currently possible.

The impact of muscles insertion points' definition on MSMs results has previously been investigated [18], future developments may consider performing a sensitivity analysis on the FEM. Finally muscle forces were estimated through a static optimization procedure, a technique

that does not account for the muscle activation experimentally recorded with superficial EMG. A study could be performed using another approach like the Computed Muscle Control method.

Despite the outlined limitations of this study, the results seem to support the hypothesis that reduced muscle function will increase internal stresses at the level of tissue and bones, thus reducing the possibility of correctly distributing PP. This can be useful in order to understand the mechanism contributing to ulcer development [8,11].

References

[1] D.G. Armstrong, A.J.M. Boulton, S.A. Bus, Diabetic foot ulcers and their recurrence, N. Engl. J. Med. 376 (June) (2017) 2367–2375, http://dx.doi.org/10.1056/NEJMra1615439.

[2] Z. Sawacha, G. Gabriella, G. Cristoferi, A. Guiotto, A. Avogaro, C. Cobelli, Diabetic gait and posture abnormalities: a biomechanical investigation through three dimensional gait analysis, Clin. Biomech. (Bristol, Avon). 24 (9) (2009) 722–728, http://dx.doi.org/10.1016/j.clinbiomech.2009.07.007.

[3] Z. Sawacha, G. Guarneri, G. Cristoferi, A. Guiotto, A. Avogaro, C. Cobelli, Integrated kinematics–kinetics–plantar pressure data analysis: a useful tool for characterizing diabetic foot biomechanics, Gait Posture 36 (1) (2012) 20–26, http://dx.doi.org/10.1016/j.gaitpost.2011.12.007.

[4] H. Andersen, P.L. Poulsen, C.E. Mogensen, J. Jakobsen, Isokinetic muscle strength in long-term IDDM patients in relation to diabetic complications, Diabetes 45 (4) (1996) 440–445.

[5] C.D. Sartor, R.H. Hasue, L.P. Cacciari, et al., Effects of strengthening, stretching and functional training on foot function in patients with diabetic neuropathy: results of a randomized controlled trial, BMC Musculoskelet Disord. 15 (2014) 137, http://dx.doi.org/10.1186/1471-2474-15-137.

[6] C. Giacomozzi, E. D'Ambrogi, S. Cesinaro, V. Macellari, L. Uccioli, Muscle performance and ankle joint mobility in long-term patients with diabetes, BMC Musculoskelet Disord. 9 (1) (2008) 99, http://dx.doi.org/10.1186/1471-2474-9-99.

[7] Z. Sawacha, F. Spolaor, G. Guarneri, et al., Abnormal muscle activation during gait in diabetes patients with and without neuropathy, Gait & Posture 35 (1) (2012) 101–105, http://dx.doi.org/10.1016/j.gaitpost.2011.08.016.

[8] P.R. Cavanagh, G.G. Simoneau, J.S. Ulbrecht, Ulceration, unsteadiness, and uncertainty: the biomechanical consequences of diabetes mellitus, J. Biomech. 26 (S1) (1993) 23–40.

[9] A. Erdemir, J.J. Saucerman, D. Lemmon, et al., Local plantar pressure relief in therapeutic footwear: design guidelines from finite element models, J. Biomech. 38 (9) (2005) 1798–1806, http://dx.doi.org/10.1016/j.jbiomech.2004.09.009.

[10] S.A. Bus, J.S. Ulbrecht, P.R. Cavanagh, Pressure relief and load redistribution by custom-made insoles in diabetic patients with neuropathy and foot deformity, Clin. Biomech. 19 (6) (2004) 629–638, http://dx.doi.org/10.1016/j.clinbiomech.2004.02.010.

[11] A. Gefen, Plantar soft tissue loading under the medial metatarsals in the standing diabetic foot, Med. Eng. Phys. 25 (2003) 491–499, http://dx.doi.org/10.1016/S1350-4533(03)00029-8.

[12] W.-M. Chen, T. Lee, P.V.-S. Lee, J.W. Lee, S.-J. Lee, Effects of internal stress concentrations in plantar soft-tissue?A preliminary three-dimensional finite element analysis, Med. Eng. Phys. 32 (4) (2010) 324–331, http://dx.doi.org/10.1016/j.medengphy.2010.01.001.

[13] A. Guiotto, Z. Sawacha, G. Guarneri, A. Avogaro, C. Cobelli, 3D finite element model of the diabetic neuropathic foot: a gait analysis driven approach, J. Biomech. 47 (12) (2014) 3064–3071, http://dx.doi.org/10.1016/j.jbiomech.2014.06.029.

[14] W.-M. Chen, J. Park, S.-B. Park, V.P.-W. Shim, T. Lee, Role of gastrocnemius?soleus muscle in forefoot force transmission at heel rise — A 3D finite element analysis, J. Biomech. 45 (10) (2012) 1783–1789, http://dx.doi.org/10.1016/j.jbiomech.2012.04.024.

[15] S.L. Delp, F.C. Anderson, A.S. Arnold, P. Loan, A. Habib, C.T. John, E. Guendelman, D.G. Thelen, OpenSim: open-source software to create and analyze dynamic simulations of movement, IEEE Trans. Biomed eng . 54 (2007) 1940–1950, http://dx.doi.org/10.1109/TBME.2007.901024.

[16] P. Saraswat, M.S. Andersen, B.A. Macwilliams, A musculoskeletal foot model for clinical gait analysis, J. Biomech. 43 (9) (2010) 1645–1652, http://dx.doi.org/10.1016/j.jbiomech.2010.03.005.

[17] J.-W. Seo, D.-W. Kang, J.-Y. Kim, et al., Finite element analysis of the femur during stance phase of gait based on musculoskeletal model simulation, Biomed. Mater. Eng. 24 (6) (2014) 2485–2493, http://dx.doi.org/10.3233/BME-141062.

[18] L. Bosmans, G. Valente, M. Wesseling, et al., Sensitivity of predicted muscle forces during gait to anatomical variability in musculotendon geometry, J. Biomech. 48 (10) (2015) 2116–2123, http://dx.doi.org/10.1016/j.jbiomech.2015.02.052.

[19] S. Del Din, E. Carraro, Z. Sawacha, et al., Impaired gait in ankylosing spondylitis, Med. Biol. Eng. Comput. 49 (7) (2011) 801–809, http://dx.doi.org/10.1007/s11517-010-0731-x.

[20] T.M. Malaquias, C. Silveira, W. Aerts, et al., Extended foot-ankle musculoskeletal models for application in movement analysis, Comput. Methods Biomech. Biomed. Eng. 20 (2) (2017) 153–159, http://dx.doi.org/10.1080/10255842.2016.1206533.

[21] A. Mantoan, C. Pizzolato, M. Sartori, Z. Sawacha, C. Cobelli, Reggiani M. MOtoNMS, A MATLAB toolbox to process motion data for neuromusculoskeletal modeling and simulation, Source Code Biol. Med. 10 (2015) 12, http://dx.doi.org/10.1186/s13029-015-0044-4.

[22] W. Aerts, F. De Groote, J. Vander Sloten, I. Jonkers, Modeling foot-ground interaction with foot surface contour and elastic foundation modeling, International Symposium on Computer Methods in Biomechanics and Biomedical Engineering (2013).

[23] H. Kura, Z.P. Luo, H.B. Kitaoka, K.N. An, Quantitative analysis of the intrinsic muscles of the foot, Anat. Rec. 249 (1) (1997) 143–151.

[24] S.K. Sarrafian, Anatomy of the Foot and Ankle Descriptive Topographic, Functional, J. B. Lippincott Company, 1983.

[25] Cheung JT-M, M. Zhang, K.-N. An, Effect of Achilles tendon loading on plantar fascia tension in the standing foot, Clin. Biomech. 21 (2) (2006) 194–203, http://dx.doi.org/10.1016/j.clinbiomech.2005.09.016.

[26] A.T.M. Phillips, P. Pankaj, C.R. Howie, A.S. Usmani, Simpson AHRW, Finite element modelling of the pelvis: inclusion of muscular and ligamentous boundary conditions, Med. Eng. Phys. 29 (7) (2007) 739–748, http://dx.doi.org/10.1016/j.medengphy.2006.08.010.

[27] E.D. Williams, M.J. Stebbins, P.R. Cavanagh, D.R. Haynor, B. Chu, M.J. Fassbind, V. Isvilanonda, W.R. Ledoux, The design and validation of a magnetic resonance imaging-compatible device for obtaining mechanical properties of plantar soft tissue via gated acquisition, Proc. Inst. Mech. Eng. H 229 (Oct (10) (2015) 732–742, http://dx.doi.org/10.1177/0954411915606150.

[28] R. Stagni, S. Fantozzi, A. Cappello, A. Leardini, Quantification of soft tissue artefact in motion analysis by combining 3D fluoroscopy and stereophotogrammetry: a study on two subjects, Clin. Biomech. 20 (3) (2005) 320–329, http://dx.doi.org/10.1016/j.clinbiomech.2004.11.012.

[29] C. Nester, R.K. Jones, A. Liu, et al., Foot kinematics during walking measured using bone and surface mounted markers, J. Biomech. 40 (15) (2007) 3412–3423, http://dx.doi.org/10.1016/j.jbiomech.2007.05.019.

[30] P.J. Antunes, G.R. Dias, A.T. Coelho, F. Rebelo, T. Pereira, Nonlinear 3D foot, FEA modeling from CT scan medical images, Comput. Vision Med. Imaging Process. (2011) 135–141.